Zygote

cambridge.org/zyg

Dynamic alterations in H4K12 acetylation during meiotic maturation and after parthenogenetic activation of mouse oocytes

Ze Zhang[1,*], Baobao Chen[2,*], Haoliang Cui[1], Haixu Gao[1], Ming Gao[1] and Chenyu Tao[1]

[1]College of Animal Science and Technology, Hebei Agricultural University, Baoding, Hebei Province, 071000 China and [2]College of Animal Science and Technology, Nanjing Agricultural University, Nanjing, Jiangsu Province, 210000 China

Research Article

Cite this article: Zhang Z *et al*. (2020) Dynamic alterations in H4K12 acetylation during meiotic maturation and after parthenogenetic activation of mouse oocytes. *Zygote*. **28**: 367–370. doi: 10.1017/S0967199420000192

Received: 16 November 2019
Revised: 7 February 2020
Accepted: 8 March 2020
First published online: 23 July 2020

Keywords:
Histone acetylation H4K12; Meiosis; Mouse; Oocyte; Parthenogenetic activation

Author for correspondence:
Chenyu Tao. College of Animal Science and Technology, Hebei Agricultural University, Baoding, Hebei Province, 071000 China.
Tel: +86 312 7528359.
E-mail: taochenyuty@163.com

*These authors contributed equally to this work.

Summary

The aim of the study was to investigate the continuous changing pattern of H4K12 acetylation, and the expression levels of histone acetyltransferases (HATs) and histone deacetyltransferases (HDACs) in mouse oocytes during meiosis and after parthenogenetic activation (PA). The immunofluorescence results showed hyperacetylation of lysine-12 on histone H4 (H4K12) in the germinal vesicle (GV) oocytes that then decreased during germinal vesicle breakdown (GVBD), and disappeared in metaphase II (MII). However, it reappeared in the early 1-cell embryos derived after 4 h of PA. The expression levels of some selected HATs and HDACs also validated the changing pattern of H4K12 acetylation during meiosis and PA. In conclusion, H4K12 is deacetylated in GVBD and MII, and re-hyperacetylated after PA.

Introduction

Recent studies have revealed that epigenetic modifications, such as DNA methylation and histone modifications, play important roles in the regulation of chromatin structure and gene expression (Shahbazian *et al.*, 2007). Two families of enzymes, histone acetyltransferases (HATs) and histone deacetyltransferases (HDACs) regulate histone acetylation.

The genomic state of oocytes is altered globally during oocyte growth and post fertilization (Panero *et al.*, 2006; Zuccotti *et al.*, 1995). A recent study reported that H4K5, H4K8, H4K12, H4K16, H3K9, and H3K14 are acetylated in mouse oocytes at the germinal vesicle (GV) stage. However, with the restart of meiosis, deacetylation occurs at all sites except for H4K8, and this state is maintained until the end of the second meiotic metaphase (MII) (Kim *et al.*, 2002).

It has been shown that acetylation of core histones is important in regulating gene expression by producing conformational changes in chromatin structure that allow DNA to be accessible to transcription factors (Long *et al.*, 2013). In addition, histone acetylation can serve as an epigenetic marker by retaining this information in the mitotic phase, and propagating it from one cell to the next generation (Jenuwein and Allis, 2001). Specifically, it was suggested that H4K12 is a critical epigenetic marker for active genes (Kruhlak *et al.*, 2001; Jin *et al.*, 2016).

The goal of this study was to determine the exact pattern of H4K12 acetylation in mouse oocytes during meiosis and after parthenogenetic activation (PA). We found that hyperacetylation decreased just after GV, was weakly detected during germinal vesicle break down (GVBD), and no signals were detected in the MII phase. However, H4K12 acetylation reappeared at the 1-cell embryos at 4 h after PA. This study reveals the dynamic alterations of H4K12 acetylation during meiotic maturation and after PA, and provides the theoretical foundation for further research into the function of acetylation during the reproductive process.

Materials and methods

Collection and culture of mouse oocyte

To obtain fully grown oocytes arrested at prophase I of meiosis, 3-week-old KunMing (KM) female mice were superovulated with 10 IU pregnant mare's serum gonadotrophin (PMSG). The ovaries were removed from the mice at 48 h post-PMSG and transferred to M2 medium (Sigma) as described previously (Sobajima *et al.*, 1993). The GV, GVBD, and MII-stage oocytes were obtained at 0 h, 4 h, and 12 h of culturing at 38.5°C and 5% CO_2 in air, at maximum humidity.

Table 1. Primers used in this study

Gene name	GenBank accession	Sequence (5′→3′)	
Gcn5	NM_020004	TTTACTTTCTCACCTATG	GATCTCTTTCTGTTTCTT
Ep300	NM_177821.6	CTCGTAAAGTGGAAGGGG	CGGATCATAGACGGGTCA
Pcaf	AF254442.1	CTAACCCCTCTCCTACTC	TCACACCCTGTTCAATAC
Hdac1	NM_008228	GCCGGGCGGCGAGCAAG	CTTGCTCGCCGCCCGGC
Hdac2	NM_008229.2	GACAAACCAGAACACTCC	AAAACTCTTCATCGCAAG
Hdac3	NM_010411	AGGAGAACTACAGCAGGC	GAGGGACAATCATCAGGC
Sirt1	AY377984.1	ACCTCTTCATATTTCGGA	ATTGTTGTTTGTTGCTTG
Sirt2	BC021439.1	AGAGGAACAGCAGTAACA	GAACGAAGGGTCTATGAG
β-actin	NM_007393.3	CATCCGTAAAGACCTCTATGCCAAC	ATGGAGCCACCGATCCACA

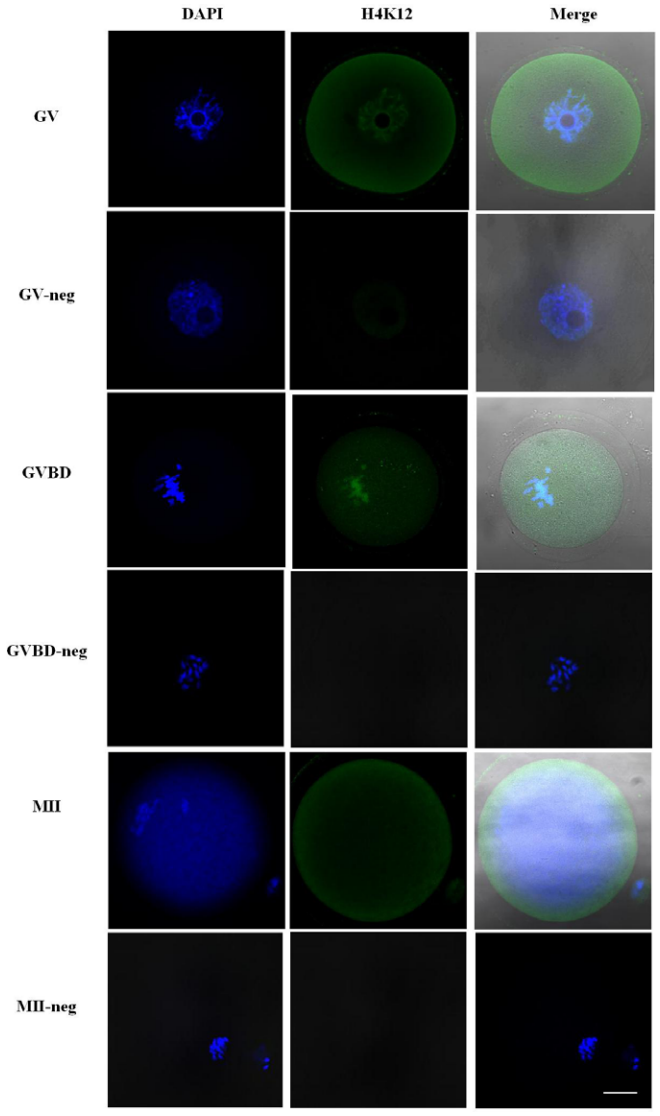

Figure 1. Immunostaining of global histone acetylation status during meiotic maturation of oocytes. GV, GVBD and MII indicate oocytes at the germinal vesicle, germinal vesicle breakdown and metaphase II stages that were stained with antibodies against AcH4K12. While GV-neg, GVBD-neg and MII-neg indicate control oocytes at the same stage, but with only the secondary antibody, and without antibodies against AcH4K12, which is shown as green. Each sample was counterstained with 4′,6-diamidino-2-phenylindole (DAPI) to visualize DNA (blue). Scale bar, 20 μm.

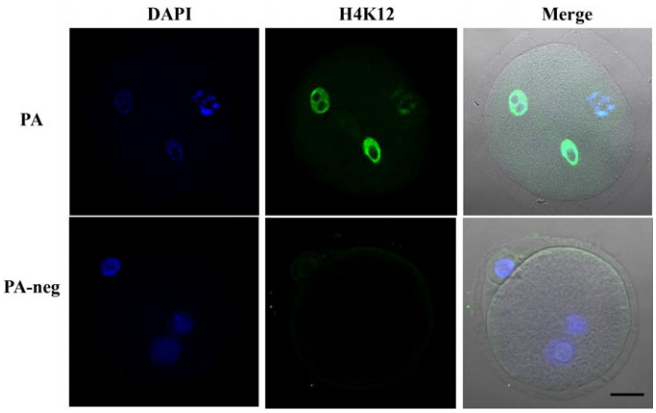

Figure 2. Immunostaining of global histone acetylation status of oocytes after parthenogenetic activation (PA). Oocytes after PA were stained with or without (PA-neg) antibodies against AcH4K12, which is shown as green; and DAPI to visualize DNA (blue). Scale bar, 20 μm.

Parthenogenetic activation

The *in vivo* matured mouse oocytes (MII oocytes) were activated by PA. These detailed procedures have been described previously (Zhang *et al.*, 2017). Briefly, the MII mouse oocytes were parthenogenetically activated by incubating in activation medium, which consisted of Ca^{2+}-free potassium-supplemented simplex optimised medium–bovine serum albumin (KSOM–BSA) supplemented with 10 mM $SrCl_2$ and 5 μg/ml cytochalasin B, at 38.5°C and 5% CO_2 in air, at maximum humidity for 6 h.

Quantitative real-time PCR

Quantitative real-time PCR (qPCR) was used to measure the relative expression of histone acetyltransferase (*Gcn5*), E1A binding protein (*Ep300*), 3-oxoadipyl-CoA thiolase (*Pcaf*), histone deacetylase 1 (*Hdac1*), histone deacetylase 2 (*Hdac2*), histone deacetylase 3 (*Hdac3*), sirtuin 1 (*Sirt1*), and sirtuin 2 (*Sirt2*) mRNA in GV, MII, and post PA oocytes. Total RNA was extracted from oocytes using the RNeasy Micro Kit (Qiagen), according to the manufacturer's protocol. Reverse transcription and qPCR were performed using the ReverTra Ace qPCR RT KitQ-PCR and SYBR Premix Ex *Taq* (TaKaRa) in a reaction volume of 20 μl and the ABI

https://doi.org/10.1017/S0967199420000192 Published online by Cambridge University Press

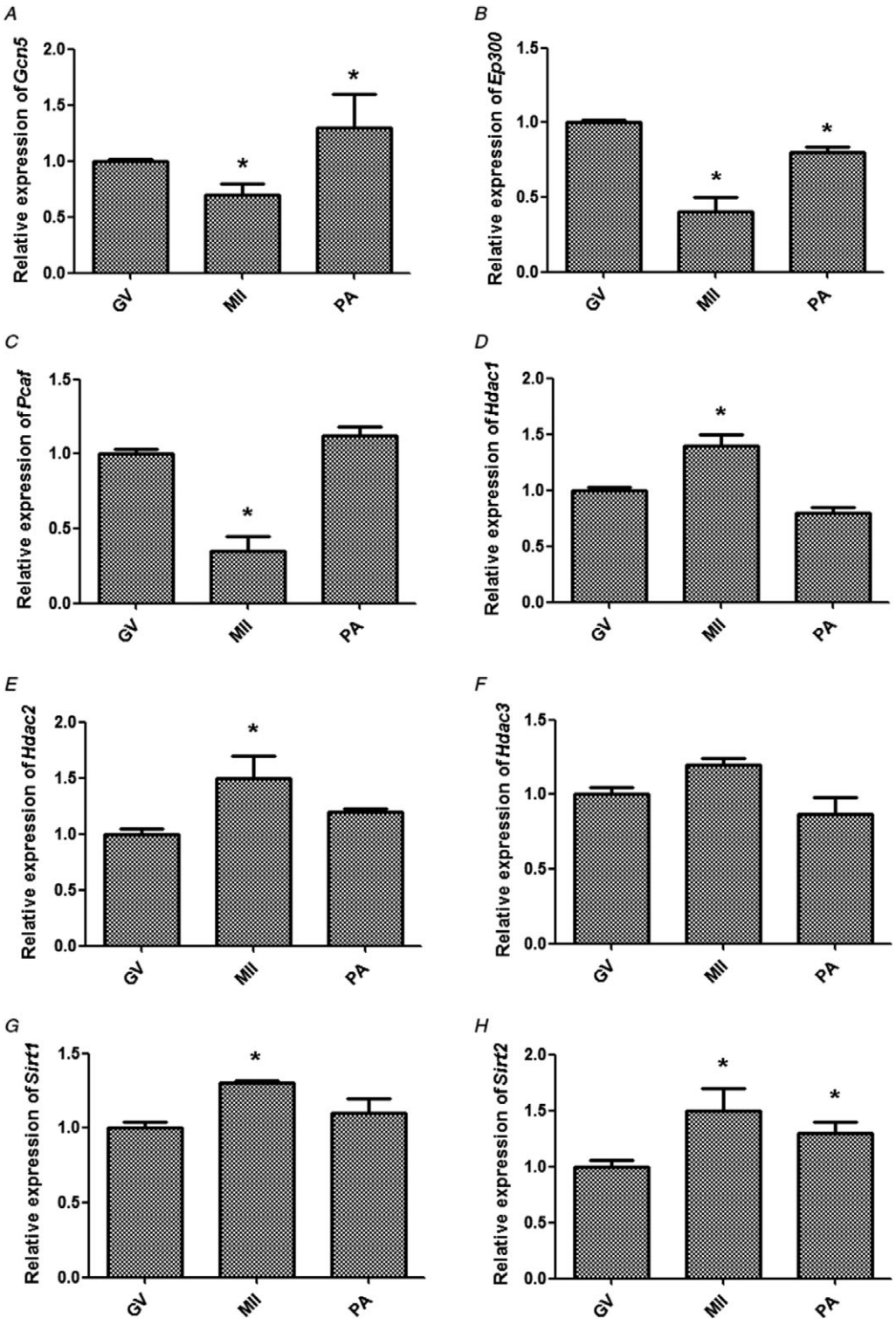

Figure 3. Relative mRNA expression of *Gcn5* (*A*), *Ep300* (*B*), *Pcaf* (*C*), *Hdac1* (*D*), *Hdac2* (*E*), *Hdac3* (*F*), *Sirt1* (*G*) and *Sirt2* (*H*) in mouse oocytes at the germinal vesicle (GV), metaphase II (MII), and after parthenogenetic activation (PA) stages (*$P < 0.05$).

StepOne system (Applied Biosystems). Each experiment was repeated four times. Primer sequences are listed in Table 1.

Immunofluorescence assay

Immunofluorescence was performed as described (Huang *et al.*, 2011). Briefly, oocytes at the GV, GVBD, MII stages and embryos were fixed in 4% (w/v) paraformaldehyde at 4°C overnight and then permeabilized with 0.5% (v:v) Triton X-100 for 30 min. After blocking in phosphate-buffered saline with 1% bovine serum albumin (PB1) for 1 h at room temperature, all samples were incubated with the primary antibodies against AcH4K12 (ab46983, Abcam) for 1 h at 37°C. After three washes in PB1 of 5 min each, oocytes were incubated with rabbit anti-mouse IgG secondary antibody (Cowin Biotech) for 1 h. After three washes, all samples were counterstained with 4′,6-diamidino-2-phenylindole (DAPI)

https://doi.org/10.1017/S0967199420000192 Published online by Cambridge University Press

(Vector Laboratories) to visualize the DNA. To confirm, the antibody we used in the experiment was specific for Lys-12 of histone H4, control experiments were carried in accordance with the same experimental protocol without using the primary antibody. Finally, fluorescence was detected using a confocal laser scanning system.

Results and discussion

H4K12 acetylation changes during meiosis

The global H4K12 acetylation status of histones during mouse oocyte maturation is shown in Fig. 1. There was an obvious GV in the middle of the GV oocyte, and H4K12 was hyperacetylated in the nucleus. However, after 4 h of maturation, the GV oocytes reached the GVBD stage, at which time the GV broke down, and H4K12 acetylation was lower than that at the GV stage. In the MII stage, the oocytes extruded the first polar body (PB1), and no fluorescence signal was detected. From the results, H4K12 is deacetylated during meiosis in mouse oocytes. Our results were consistent with the finding of Aoki's group that H4K12 is deacetylated when oocytes enter the first meiotic phase, temporarily acetylated around the time of completion of the first meiosis, and then deacetylated again when the oocytes enter the second meiotic phase (Akiyama *et al.*, 2004).

H4K12 acetylation distribution in oocytes after 4-hour-PA

The MII oocytes were then subjected to PA using $SrCl_2$ and cytochalasin B, and the H4K12 acetylation distribution is shown in Fig. 2. The oocytes had formed two pronuclei after 4 h of PA, shown on the left-hand side of Fig. 2. Our results also showed that H4K12 acetylation reappeared after PA. There have been a few studies on the changes in acetylation after PA until now. However, some research on the changes in acetylation after fertilization has been published, showing that acetylation of histones occurs in both male and female pronuclei (Kageyama *et al.*, 2007).

Relative mRNA expression of several representative HDACs and HATs

As histone acetylation levels are closely related to levels of HDACs and HATs, we selected three HAT genes, *Gcn5*, *Ep300*, and *Pcaf*, and five HDAC genes, *Hdac1*, *Hdac2*, *Hdac3*, *Sirt1*, and *Sirt2*, and measured their gene expression levels in the oocytes at GV and MII stages, and at 4 h after PA. The results are shown in Fig. 3. Expression levels of *Gcn5*, *Ep300*, and *Pcaf* all decreased significantly in MII compared with GV, and had an increasing trend from MII to PA [mean ± standard error of the mean (SEM) relative expression of *Gcn5*: 0.70 ± 0.10 at metaphase MII and 1.27 ± 0.31 at PA; *Ep300*: 0.41 ± 0.09 at MII and 0.80 ± 0.04 at PA; and *Pcaf*: 0.35 ± 0.12 at MII and 1.12 ± 0.06 at PA; $P < 0.05$]. All five selected HDAC genes showed a significant increase in MII compared with that in the GV, while the expression levels in PA declined and were similar to those in the GV (mean ± SEM relative expression of *Hdac1*: 1.41 ± 0.10 at metaphase MII and 0.79 ± 0.05 at PA; *Hdac2*: 1.50 ± 0.19 at MII and 1.21 ± 0.03 at PA; *Hdac3*: 1.19 ± 0.04 at MII and 0.87 ± 0.11 at PA; *Sirt1*: 1.32 ± 0.02 at MII and 1.11 ± 0.09 at PA; *Sirt2*: 1.50 ± 0.21 at MII and 1.31 ± 0.11 at PA; $P < 0.05$). The same genes were selected in a previous study to investigate the changes in the expression levels in GV, MI, and MII oocytes from control and diabetic mice (Ding *et al.*, 2012). The difference between the control and diabetic mice oocytes was reported, but the changing pattern of these genes in control oocytes was not described, which we have done in this study. The expression levels of these genes matched the immunostaining results.

Financial support. This work was supported by the National Natural Science Foundation of China (31802063), the Youth Foundation of Hebei Educational Committee (2018166) and Scientific Research Foundation for the Introduction of Talent in Hebei Agricultural University (ZD201718).

Conflicts of interest. The authors declare no conflicts of interest.

Ethical standards. All experiments were performed in accordance with the guide for the Care and Use of Laboratory Animals prepared by the Institutional Animal Care and Use Committee of Hebei Agricultural University, China.

References

Akiyama T, Kim JM, Nagata M and Aoki F (2004). Regulation of histone acetylation during meiotic maturation in mouse oocytes. *Mol Reprod Dev* **69**, 222–7.

Ding L, Pan R, Huang X, Wang JX, Shen YT, Xu L, Zhang Y, Liu Y, He XQ, Yang XJ, Qi ZQ and Wang H (2012). Changes in histone acetylation during oocyte meiotic maturation in the diabetic mouse. *Theriogenology* **78**, 784–92.

Huang X, Wang HL, Qi ST, Wang ZB, Tong JS, Zhang QH, *et al.* (2011). DYNLT3 is required for chromosome alignment during mouse oocyte meiotic maturation. *Reprod Sci* **18**, 983–9.

Jenuwein T and Allis CD (2001). Translating the histone code. *Science* **293**, 1074–80.

Jin L, Zhu HY, Guo Q, Li XC, Zhang YC, Zhang GL, Xing XX, Xuan MF, Luo QR, Yin XJ and Kang JD (2016). PCI-24781 can improve in vitro and in vivo developmental capacity of pig somatic cell nuclear transfer embryos. *Biotechnol Lett* **38**, 1433–41.

Kageyama S, Liu H, Kaneko N, Ooga M, Nagata M and Aoki F (2007). Alterations in epigenetic codifications during oocyte growth in mice. *Reproduction* **133**, 85–94.

Kim J-M, Ogura A, Nagata M and Aoki F (2002). Analysis of the chromatin remodeling in the embryos reconstructed by somatic nuclear transfer. *Biol Reprod* **67**, 760–6.

Kruhlak MJ, Hendzel MJ, Fischle W, Bertos NR, Hameed S, Yang X-J, Verdin E and Bazett-Jones DP (2001). Regulation of global acetylation in mitosis through loss of histone acetyltransferases and deacetylases from chromatin. *J Biol Chem* **276**, 38307–19.

Long H, Lu SS, Kuang YP, Yan ZG, Liang HX, Yu S, Chai WR, Yan Z and Lyu QF (2013). Incubation of sperm heads impairs fertilization and early embryo development following intracytoplasmic sperm injection (ICSI) by decreasing oocyte activation in mice. *Biotechnol Lett* **35**, 1823–9.

Panero J, Trelles J, Rodano V, Montserrat JM, Iglesias LE, Lewkowicz ES and Iribarren AM (2006). Microbial hydrolysis of acetylated nucleosides. *Biotechnol Lett* **28**, 1077–81.

Shahbazian MD and Grunstein M (2007). Functions of site-specific histone acetylation and deacetylation. *Annu Rev Biochem* **76**, 75–100.

Sobajima, Aoki F and Kohmoto K (1993). Activation of mitogen-activated protein kinase during meiotic maturation in mouse oocytes. *J Reprod Fertil* **97**, 389–94.

Zhang YC, Jin L, Zhu HY, Guo Q, Li XC, Zhang GL, Xing XX, Xuan MF, Luo QR, Luo ZB, Wang JX, Cui CD, Li WX, Cui ZY, Yin XJ and Kang JD (2017). The developmental competence of oocytes parthenogenetically activated by an electric pulse and anisomycin treatment. *Biotechnol Lett* **39**, 189–96.

Zuccotti M, Piccinelli A, Giorgi Rossi P, Garagna S and Redi CA (1995). Chromatin organization during mouse oocyte growth. *Mol Reprod Dev* **41**, 479–85.

https://doi.org/10.1017/S0967199420000192 Published online by Cambridge University Press